18

Aerodynamic Parameters on a Multisided Cylinder for Fatigue Design

Byungik Chang
West Texas A&M University
USA

1. Introduction

Cantilevered signal, sign, and light support structures are used nationwide on major interstates, national highways, local highways, and at local intersections for traffic control purposes. Recently, there have been a number of failures of these structures that can likely be attributed to fatigue. In Iowa, USA (Dexter 2004), a high-mast light pole (HMLP), which is typically used at major interstate junctions, erected for service in 2001 along I-29 near Sioux City collapsed in November 2003 (see Figure 1 (a)). Fortunately, the light pole fell onto an open area parallel to the interstate and injured no one. Figure 1 (b) shows another high-mast lighting tower failure in Colorado, USA (Rios 2007) that occurred in February of 2007. Similar to the failure in South Dakota, fracture initiated at the weld toe in the base plate to pole wall connection, and then propagated around the pole wall until the structure collapsed. It appears that these structures may have been designed based on incomplete and/or insufficient code provisions which bring reason to reevaluate the current codes that are in place.

A luminary support structure or HMLP is generally susceptible to two primary types of wind loading induced by natural wind gusts, or buffeting and vortex shedding, both of which excite the structure dynamically and can cause fatigue damage (AASHTO 2009). Vortex shedding is a unique type of wind load that alternatively creates areas of negative pressures on either side of a structure normal to the wind direction. This causes the structure to oscillate transverse to the wind direction. When the vortex shedding frequency (i.e., the frequency of the negative pressure on one side of the structure) approaches the natural frequency of the structure, there is a tendency for the vortex shedding frequency to couple with the frequency of the structure (also referred to as "lock-in" phenomenon) causing greatly amplified displacements and stresses.

2. Background and objectives

While vortex shedding occurs at specific frequencies and causes amplified vibration near the natural frequencies of the structure, buffeting is a relatively "broad-band" excitation and includes frequencies of eddies that are present in the natural wind (usually up to 2 Hz) as well as those caused by wind-structure interactions. The dynamic excitation from buffeting can be significant if the mean wind speed is high, the natural frequencies of the structure are below 1 Hz, the wind turbulence intensity is high with a wind turbulence that is highly

Fig. 1. A collapsed high-mast light pole; (a) Iowa (Dexter 2004), (b) Colorado (Rios 2007)

correlated in space, the structural shape is aerodynamically odd with a relatively rough surface, and the mechanical damping is low. In practice, a structure is always subject to both vortex shedding and buffeting excitations. But unlike vortex shedding, where amplified dynamic excitation occurs within a short range of wind speeds, buffeting loads keep increasing with higher wind speeds.

For multisided slender support structures, the current American Association of State Highway and Transportation Officials (AASHTO) Specification does not provide all the aerodynamic parameters such as the static force coefficients, their slopes with angle of attack, Strouhal number, the lock-in range of wind velocities and amplitude of vortex-induced vibration as a function of Scruton number, etc, that are needed for proper evaluation of aerodynamic behavior. Thus, wind tunnel testing was required to obtain these parameters. Buffeting, self-excited and vortex shedding responses are those significant parameters in the design of a slender support structure.

A number of experimental and theoretical investigations have been made by Peil and Behrens (2002) to obtain a realistic basis for a reliable and economic design for lighting and traffic signal columns. The investigations were based on a nonlinear spectral approach which is confined to the correlated parts of the wind turbulence and the associated wind forces. Gupta and Sarkar (1996) conducted wind tunnel tests on a circular cylinder to identify vortex-induced response parameters in the time domain. Chen and Kareem (2000, 2002) worked on modeling aerodynamic phenomena, buffeting and flutter, in both time and frequency domains, and Scanlan (1984, 1993), Caracoglia and Jones (2003), Zhang and Brownjohn (2003), and Costa (2007) and Costa and Borri (2006) studied the aerodynamic indicial function for lift and admittance functions for structures. Together this collection of work provides the motivation for the model discussed herein. The effects of aerodynamic coupling between the buffeting and flutter responses have been addressed by past studies based on the theoretical expression. The aerodynamic admittance function for lift of a thin symmetrical airfoil, known as Sears function, was theoretically derived by Sears (1941), and a somewhat simpler form of the Sears function was suggested by Liepmann (1952). Jancauskas (1983) and Jancauskas and Melbourne (1986) verified the Sears' theoretical plot experimentally for an airfoil and suggested a simplified but approximate expression. An empirical function for aerodynamic admittance for drag on a square plate was developed by Vickery (1965) based on limited experimental data. In previous research, Skop and Griffin (1975) derived an empirical formula to predict the maximum displacement amplitude for a circular cylinder based on Scruton numbers. Repetto and Solari (2004) developed an analytical model based on frequency-domain methods and quasi-steady theory to determine the along-wind and across-wind fatigue estimation of urban light pole. This model considers all modes of vibration and thereby avoids overestimation of base stress and underestimation of top displacement of the slender support structure.

3. Wind tunnel testing

The primary objective of this study is to develop aerodynamic parameters for multisided shapes. To be able to calculate the needed data for the structure, many wind parameters, such as the static drag coefficient, the slope of aerodynamic lift coefficient, Strouhal number, the lock-in range of wind velocities producing vibrations, and variation of amplitude of vortex-induced vibration with Scruton number, are needed. From wind tunnel experiments, aerodynamic parameters were obtained for an octagonal shape structure. Even though aerodynamic coefficients are known from past test results, they need to be refined by conducting further wind tunnel tests.

The use of wind tunnels to aid in structural design and planning has been steadily increasing in recent years (Liu 1991). Kitagawa et al. (1997) conducted a wind tunnel experiment using a circular cylinder tower to study the characteristics of the across-wind response at a high wind speed. The authors found from the tests that both the vortex induced vibration at a high wind speed and the ordinary vortex induced vibration were observed under uniform flow.

Bosch and Guterres (2001) conducted wind tunnel experiments to establish the effects of wind on tapered cylinders using a total of 53 models representing a range of cross sections, taper ratios, and shapes (circular, octagonal, or hexagonal cross section), which were intended to be representative of those commonly found in highway structures. In a test of drag coefficient versus Reynolds number for the uniform circular cylinders, the results

showed a consistent trend of convergence with a range of Reynolds numbers for which the drag coefficient flattens out to a constant value. It was also found that the introduction of a taper ratio significantly altered the aerodynamic behavior of the cylinder shapes. Wind tunnel experiments by James (1976) were performed to establish the effects of wind on uniform cylinders using several models representing a range of shapes (octagonal, dodecagonal and hexdecagonal cross section), model orientations, and corner radii based on Reynolds number (Re) between 2.0×10^5 and 2.0×10^6. Lift and drag coefficients were developed for an octagonal cylinder by Simui and Scanlan (1996). In the study, the slope of the mean drag coefficient (C_D) was found to be near zero and the slopes of the mean lift coefficient (C_L) were calculated to be approximately -1.7π for flat orientation and 0.45π for corner orientation.

Wind tunnel testing is routinely used to study various aerodynamic phenomena and determine aerodynamic parameters of civil engineering structures. Also, the general flow pattern around structures can be determined from wind tunnel testing, particularly in the case of unusual structural shapes. Wind tunnel testing aids in structural design and planning because required aerodynamic coefficients may not always be available in codes or standards (Liu, 1991).

3.1 Wind tunnel and test models

The wind tunnel that was used for this study is the Bill James Open Circuit Wind Tunnel (see Figure 2), which is located in the Wind Simulation and Testing Laboratory (WiST Lab) at Iowa State University (ISU), Ames, USA. This is a suction orientation wind tunnel with a 22:1 contraction ratio. The wind tunnel test section is of the dimensions 3ft x 2.5ft and 8ft length following the contraction exit. The test section has an acrylic viewing window next to the wind tunnel control/data station with an access door opposite the side of the station. The fan, which is located downstream of the test section, is powered by a 100hp, 3-phase, 440 volt motor. The fan is controlled either by an analog remote control knob which is located at the wind tunnel control station and connected to the variable frequency fan, or directly by using the digital control screen mounted on the actual motor control power box. The fan speed can be changed in minimal steps of 0.1 Hz or approximately 0.51 ft/s (0.16 m/s) using these controls.

For all of the tests, a wooden cylindrical model with an octagonal (8-sided) and a dodecagonal (12-sided) cross section of diameter 4 in. (flat to flat distance) and length of 20 in. were used. These dimensions were selected based on the need to maintain a wind tunnel blockage criterion of 8% or less. The actual blockage was 7.4% and, therefore, blockage effects could be neglected. The length of the model, 20 inches, was chosen to maximize the area of the model that would be exposed to the air stream while at the same time leaving enough room on both sides of the model to attach any additional fixtures that are required in order to change certain parameters.

End plates, which are made out of clear plastic, were attached to the model to minimize the three-dimensional end effects on the model and to, in turn, maintain a two-dimensional flow on the model. To test multiple modifications of the model with a different mass, pairs of commercially available C clamps were clamped to the end plates at equal distances from the centerline of the model to avoid any torsion.

3.2 Static tests

For the static tests, each model was fixed horizontally in the wind tunnel with zero yaw angle and the aerodynamic forces were measured at various wind speeds. The angle of

attack was varied by rotating the model about its longitudinal axis. Wind speeds were carefully chosen to provide a large range of Reynolds numbers. The load cells for this system were fixed to the test frame as shown in the figure. Thin strings were attached to the aluminum block at each end of the model to avoid vertical deflection of the model.

The wind speeds in this test were varied from 0.6 to 30.5 m/s (2 to 100 ft/s) to yield a range of Reynolds Number (Re) from 2.5×10^4 to 2.3×10^5. The drag coefficients, C_D were calculated from the mean drag force and variable mean wind speeds using the following equation.

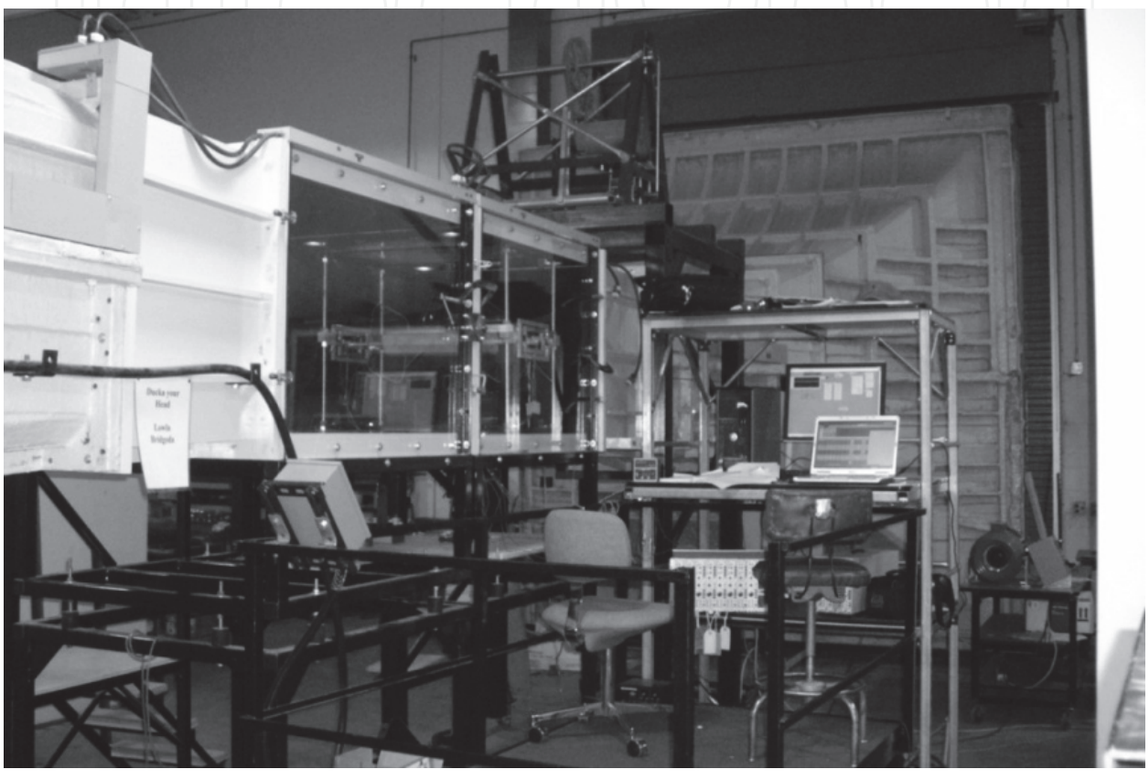

Fig. 2. Bill James Wind Tunnel at Iowa State University

$$C_D = \frac{F_D}{\frac{1}{2} \cdot \rho \cdot U^2 \cdot A} \tag{1}$$

where F_D = mean drag force; ρ = air density; U = mean wind speed; and A = projected area of model (= D ·L).

To verify the force-balance system, drag coefficients for a circular cylinder was measured at several Re and compared with other references. The average difference of drag coefficient measured with respect to other reference values for Re varying between 4.0×10^4 and 1.0×10^5 was approximately 2.3 %.

Figure 3 presents C_D versus Re for the uniform dodecagonal shape cylinder. In this plot, it can be observed that the C_D for the cylinder with corner orientation increases until Re equals approximately 1.5×10^5, beyond which it tends to converge to 1.45. With flat orientation, the C_D appears to stabilize at 1.56 at approximately the same Re. The static

tests indicated that the angle of attack (α) of the wind on the cylinder influences the C_D and also showed that the flat orientation results in a slightly higher C_D than those for the corner orientation.

According to Scruton (1981), the drag coefficients for a dodecagonal shape with flat orientation are 1.3 in the subcritical region and 1.0 in the supercritical region. James (1976) also conducted several wind tunnel tests to measure drag and lift coefficients on various polygon shaped cylinders. For a dodecagonal shape with sharp corners, James found the drag coefficient as 1.3 and 1.2 for flat and corner orientation, respectively, in Re varying from 3.0×10^5 to 2.0×10^6. Based on their research, drag coefficients of 1.2 and 0.79 for subcritical and supercritical region, respectively, are prescribed in the current AASHTO Specification and used for design. It is noted that the drag coefficients of 1.45 and 1.56 for both the orientations of the dodecagonal shape, as measured in the ISU Bill James Wind Tunnel for the sub-critical region, are higher than the value of 1.2 used currently for design."

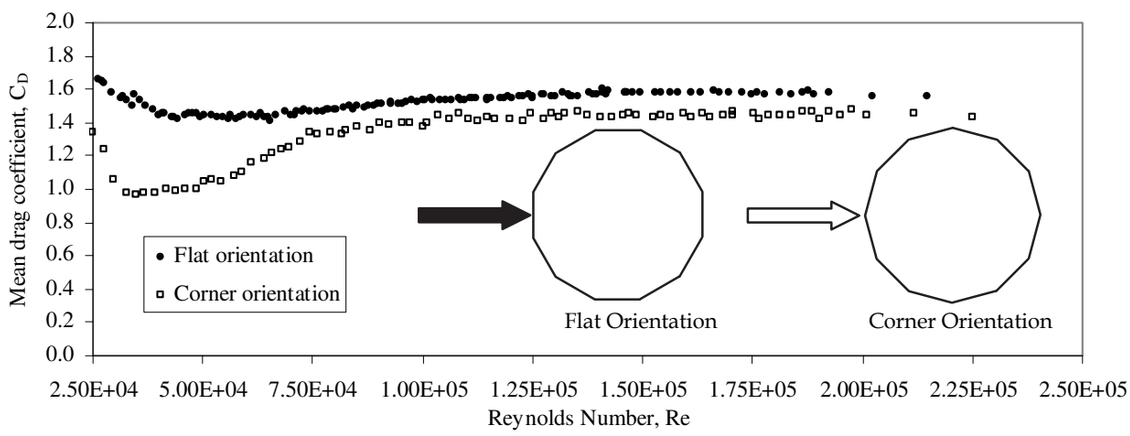

Fig. 3. Mean drag coefficients (C_d) for a dodecagonal cylinder.

A similar force-balance system was used to obtain lift force in the static tests. The model was fixed in the vertical direction perpendicular to the air flow in the wind tunnel. The mean lift coefficients (C_L) were calculated from the mean lift force and mean wind speed using the following equation.

$$C_L = \frac{F_L}{\frac{1}{2}\cdot\rho\cdot U^2\cdot A} \tag{2}$$

where F_L = mean lift force.

The slopes of C_L with respect to the angle of attack, $dC_L/d\alpha$, were calculated to be approximately -0.7π and 0.5π for flat- and corner-orientation, respectively. The Re varied from 9.3×10^4 to 1.6×10^5 in these tests (see Figure 4).

3.3 Dynamic tests

Many tests were conducted on the models to obtain all of the needed aerodynamic parameters. Results of most importance include Strouhal number (St), lock-in range of wind

velocities for vortex shedding, and the amplitude of vortex-induced vibrations as a function of the Scruton number (Sc).

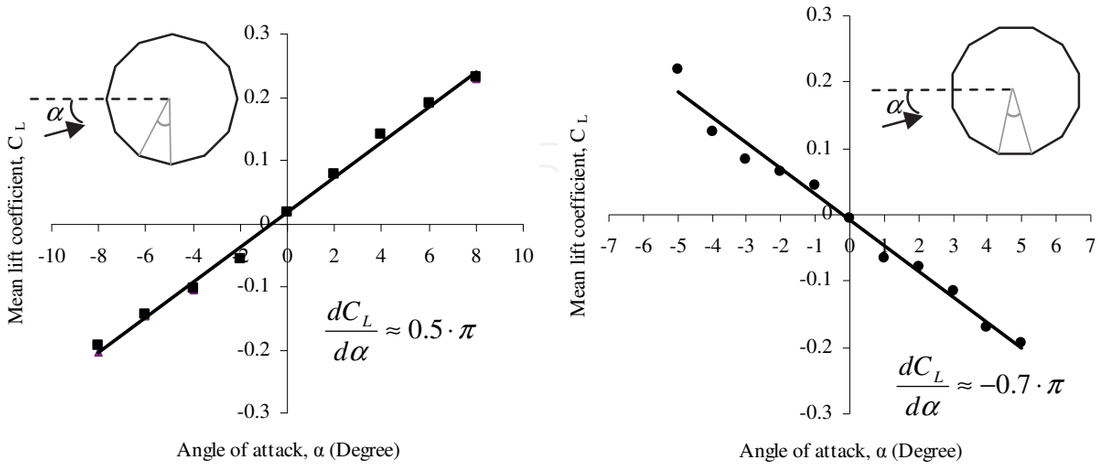

(a) Flat orientation (b) Corner orientation

Fig. 4. Lift coefficient (C_L) and its slope for the dodecagonal cylinder.

For the dynamic test, the vertical motion dynamic setup was designed to allow only a single-degree-of-freedom, which means that the test model was designed to only allow motion along the vertical axis perpendicular to the wind direction. Each model was suspended by a set of eight linear coil springs and chains, with four of each on each side of the model. Two cantilever type force transducers were used with one placed at the top and one at the bottom, at diagonally opposite springs.

Spring Suspension System

The spring suspension system was attached to a frame that was fixed to the test section floor and ceiling immediately adjacent to the side walls. A load cell frame was constructed with small structural channels and four 0.75 inch diameter threaded steel walls with two on each side of the test section which spanned vertically from the floor to the ceiling of the test section. Figure 5 shows a schematic diagram of the dynamic test suspension system.

Lock-in range and Strouhal number

The lock-in range and Strouhal number ($f_s \cdot D/U \approx 0.17$ and 0.2 for a 8-sided and 12-sided shape respectively) were determined based on the dynamic tests. Lock-in occurs when the vortex shedding frequency matches the natural frequency of the actual system which occurs at a critical wind speed causing the response at the lock-in region to be much larger than that of the normal region. The lock-in region stays consistent over a certain range of wind speeds. Figure 6 shows the frequency spectrum of the displacement response of the elastically supported cylinder for the three different instances of (a) before lock-in, (b) at lock-in, and (c) after lock-in, all for the flat orientation, where f_s and f_n are the vortex-shedding frequency and the natural frequency, respectively, of the test model. These figures show that the model produces much higher amplified displacements when the vortex shedding frequency and the natural frequency match one another.

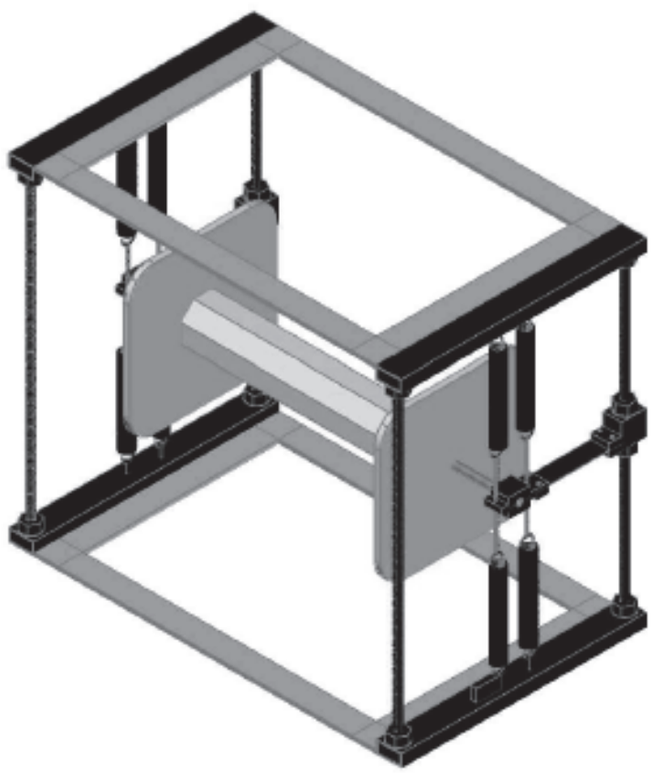

Fig. 5. Schematic diagrams of the dynamic suspension system

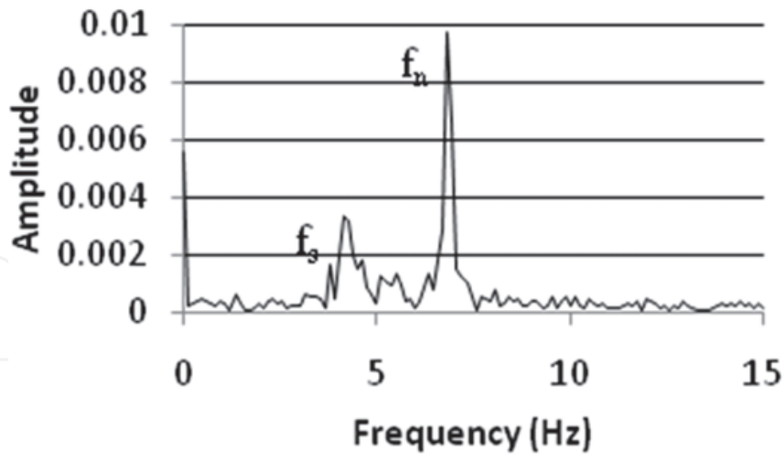

(a) before lock-in

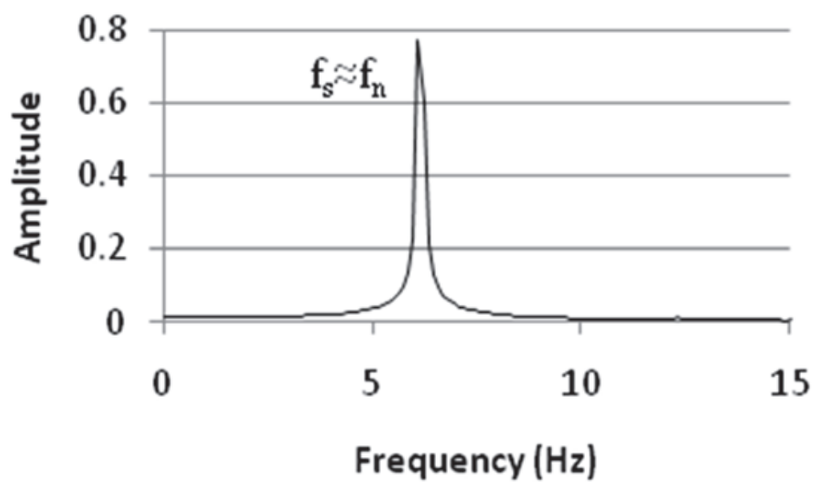

(b) at lock-in

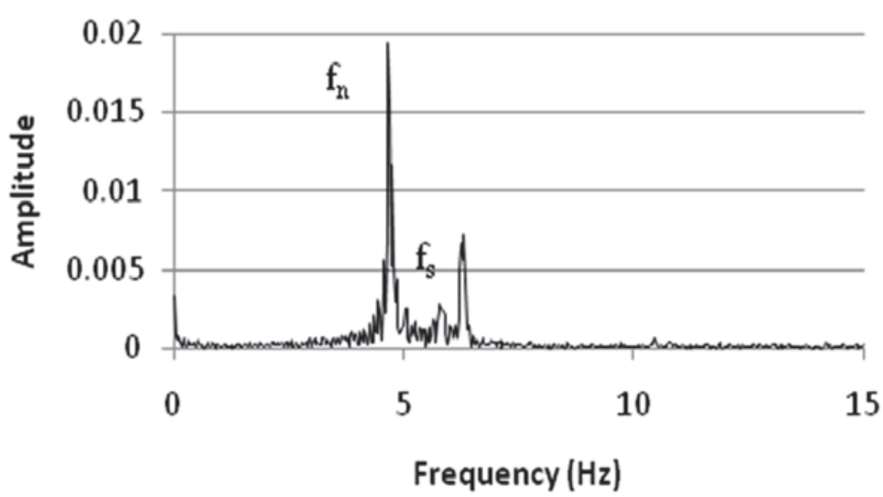

(c) after lock-in

Fig. 6. Frequency spectra of displacement response of the octagonal cylinder

Scruton number

The amplitude of the model is directly related to the Scruton number (S_c). In order to determine the amplitude versus the S_c, it was necessary to obtain several different parameters. These parameters include the inertial mass, stiffness, natural frequency, and the system damping ratio. The S_c is solved using the following:

$$S_c = \frac{m \cdot \zeta}{\rho \cdot D^2}, \tag{3}$$

where m = mass per unit length; ζ = critical damping ratio; ρ = flow density; and D = cross-wind dimension of the cross-section.

The inertial mass, stiffness, and natural frequency for each case were determined using the added mass method, by adding masses incrementally. This was done by testing multiple specimens of the model with different masses, added by clamping pairs of commercially available C-clamps with different weights to the previously described plastic end plates. A total of five pairs of clamps and one thin steel plate were used. To avoid the introduction of torsion on the testing model, the clamps and the steel plate were added to the plastic end plates on opposite sides of the cylinder. The system damping was determined for each case experimentally by using the logarithmic decrement method.

The S_c for each case of added mass was calculated using Eq. 3 and the reduced amplitude (y_o/D, max amp./diameter of the model) was obtained from the measurement that was taken when the maximum displacement occurred. The best fit line was also plotted and is shown in Figure 7.

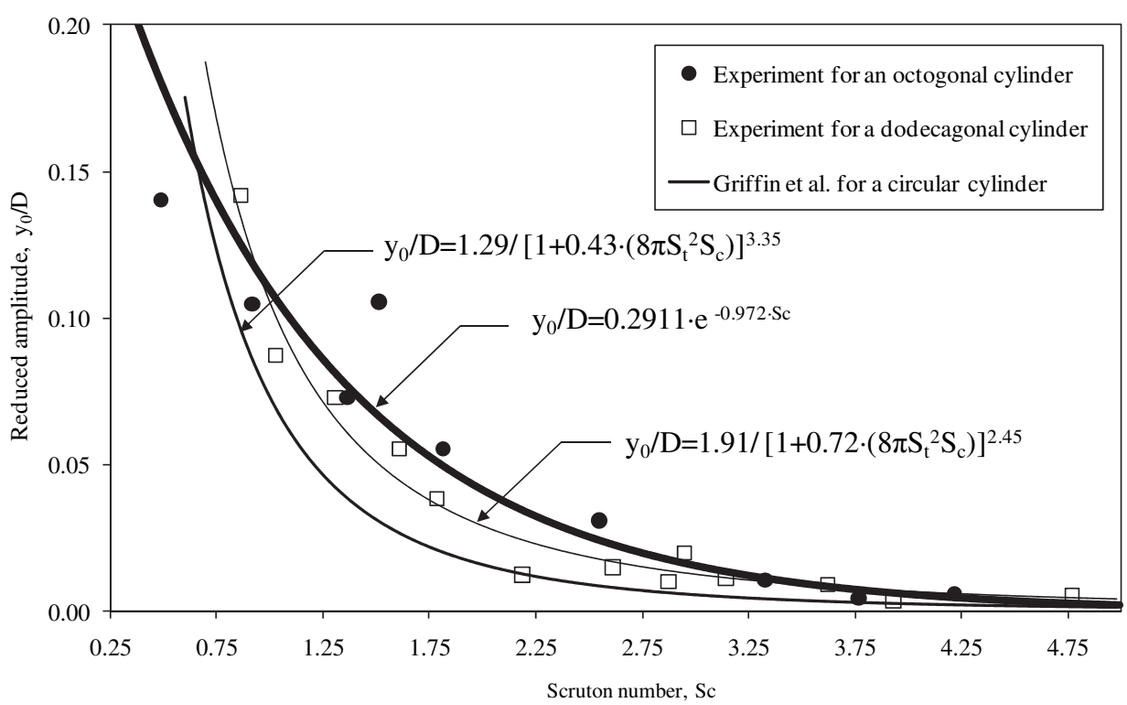

Fig. 7. Scruton number vs. maximum amplitude

3.4 Buffeting test

The relationship in the frequency domain between the power spectral density of turbulence in the upstream flow and the power spectral density of fluctuating wind load that it induces on a structure can be defined in terms of an aerodynamic admittance that is a function of the reduced frequency. A similar relationship in the time domain can be defined in terms of buffeting indicial functions. Generally, these relationships need to be determined experimentally since the flow around a structure in turbulent wind is too complex to be derived analytically.

These are also referred as impulse response functions (Chen and Kareem 2002) and counterparts of the indicial functions that are used to define the aeroelastic forces. Generally, these relationships need to be determined experimentally since the flow around a structure in turbulent wind is too complex to be handled analytically. For a dodecagonal cylinder, the aerodynamic admittance functions for drag and lift forces were obtained experimentally from static wind-tunnel model tests.

To accomplish this, a gust generator was fixed upstream of the model to generate a sinusoidal gust, with vertical and horizontal velocity fluctuations, at a fixed frequency. This device is made up of two thin airfoils with a gap of 203 mm (8 in.) between them. The airfoils are linked together and driven by a set of levers attached to a step motor. The gust generator system was placed at an upstream distance of 152 mm (6 in.) from the front surface of the cylinder and could oscillate with a maximum amplitude of approximately ±6 degree to produce the wind gust. An x-hot-wire probe was used to obtain the horizontal and vertical wind velocity fluctuations and force transducers were used to simultaneously measure the aerodynamic lift or drag on the model. The hot-wire x-probe was placed along the centerline of the model between the model and the gust generator. The buffeting indicial functions for drag and lift forces were derived from the obtained aerodynamic admittance functions. The power spectral density functions for the buffeting forces in along-wind and lateral-wind directions are follows:

$$S_{F_b^x F_b^x}(n) = (\frac{1}{2} \cdot \rho \cdot U^2 \cdot A \cdot C_D)^2 \cdot \frac{4 \cdot S_{uu}(n)}{U^2} \cdot \chi_u^2(n) \tag{4}$$

$$S_{F_b^y F_b^y}(n) = [\frac{1}{2} \cdot \rho \cdot U^2 \cdot A \cdot (C_D + \frac{dC_L}{d\alpha})]^2 \cdot \frac{4 \cdot S_{ww}(n)}{U^2} \cdot \chi_w{}^2(n) \tag{5}$$

Where, $S_{F_b^x F_b^x}(n)$ and $S_{F_b^y F_b^y}(n)$ = power spectral density function for the along and lateral buffeting forces, respectively, $S_{uu}(n)$ and $S_{ww}(n)$ = power spectral density function for the along and lateral-wind velocity fluctuations respectively, and $\chi_u^2(n)$ and $\chi_w{}^2(n)$ = aerodynamic admittance function for along and lateral forces, respectively.

Figure 8 shows the aerodynamic admittance functions calculated from the buffeting wind-tunnel tests. The frequency of the gust generator and the wind speed were both chosen to obtain a range of the reduced frequency (K) from 0.005 to 1.5. Specifically, the frequency of the gust generator ranged from approximately 0.2 to 4 Hz while the wind velocity varied approximately 5 to 65 ft/s (1.5 to 19.8 m/s).

4. Conclusion

The objective of the work presented here was to develop a universal model for predicting buffeting, self-excited and vortex shedding induced response of a slender structure in time domain for fatigue design. To accomplish this, wind tunnel tests of the multisided cross section to extract its aerodynamic properties was used as inputs in the coupled dynamic equations of motion for predicting the wind-induced response.

The wind tunnel tests on section models of the HMLP cross section (8 and 12-sided cylinders) were conducted in the Bill James Wind Tunnel in the WiST Laboratory at Iowa State University. Finally, the dynamic models that were developed for predicting the wind-excited response was validated by comparing the simulation results, obtained with aerodynamic parameters and wind speed parameters measured in wind tunnel and field, respectively, with the data collected in the field. The study contributes to the procedure for the extraction of indicial functions that define the buffeting forces and their actual forms in addition to systematically finding other aerodynamic parameters of a 12-sided cylinder.
The following conclusions can be drawn based on the current work as presented in this paper:

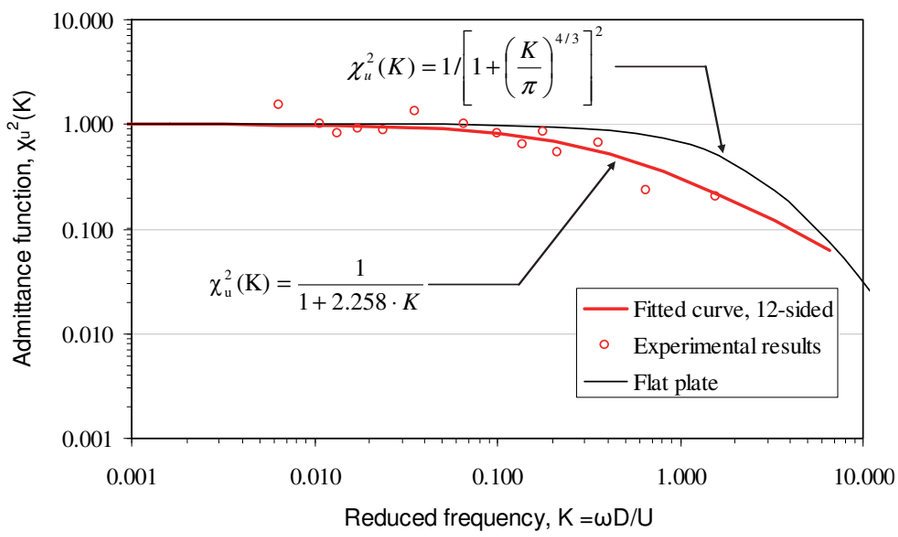

(a) Along-wind admittance function (χ_u^2)

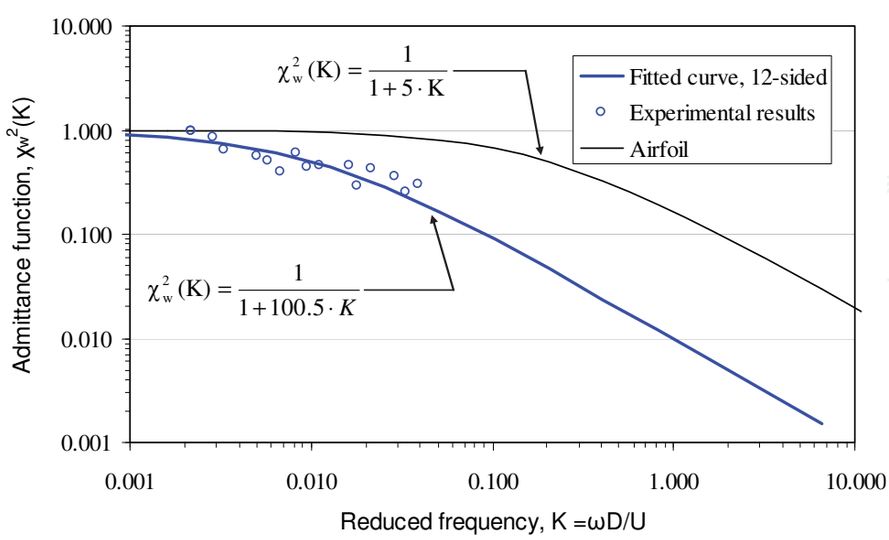

(b) Lateral-wind admittance function (χ_w^2)

Fig. 8. Aerodynamic admittance functions for a dodecagonal cylinder

5. References

American Association of State Highway and Transportation Officials (AASHTO). (2001). Standard specifications for structural support for highway signs, luminaries, and traffic signals, Washington, D.C.

Bosch, H.R. and Guterres, R. M. (2001). Wind tunnel experimental investigation on tapered cylinders for highway support structures. *Journal of wind Engineering and Industrial Aerodynamics*, 89, 1311-1323.

Caracoglia, L., and Jones, N. P. (2003). Time domain vs. frequency domain characterization of aeroelastic forces for bridge deck sections. *J. Wind. Eng. Ind. Aerodyn.*, 91, 371-402.

Chen, X., and Kareem, A. (2000). Time domain flutter and buffeting response analysis of bridges. *J. Eng. Mech.*, 126(1), 7-16.

Chen, X., and Kareem, A. (2002). Advances in modeling of aerodynamic forces on bridge decks. *J. Eng. Mech.*, 128(11), 1193-1205.

Costa, C. (2007). Aerodynamic admittance functions and buffeting forces for bridges via indicial functions. *J. Fluids and Struct.*, 23, 413-428.

Costa, C., and Borri, C. (2006). Application of indicial functions in bridge deck aeroelasticity. *J. Wind Eng. Ind. Aerodyn.*, 94, 859-881.

Dexter, R. J. (2004). Investigation of Cracking of High-Mast Lighting Towers. Final Report, Iowa Department of Transportation, Ames, IA.

Gupta, H., and Sarkar, P. P. (1996). Identification of vortex-induced response parameters in time domain. *J. Eng. Mech.*, 122(11), 1031-1037.

Henry Liu, Wind Engineering, Prentice Hall, New Jersey, 1991

James, W. D. (1976). Effects of Reynolds number and corner radius on two-dimentional flow around octagonal, dodecagonal and hexdecagonal cylinder, Doctoral dissertation, Iowa State University, Ames, Iowa.

Jancauskas, E. D. (1983). The cross-wind excitation of bluff structures and the incident turbulence mechanism, Doctoral dissertation, Monash Univ., Melbourne, Australia.

Jancauskas, E. D., and Melbourne, W. H. (1986). The aerodynamic admittance of two-dimensional rectangular section cylinders in smooth flow. *J. Wind. Eng. Ind. Aerodyn.*, 23 (1986) 395-408.

Kitagawa, Tetsuya et al. (1997), An experimental study on vortex-induced vibration of a circular cylinder tower at a high wind speed. *Journal of wind Engineering and Industrial Aerodynamics*, 69-71, 731-744.

Liepmann, H. W. (1952). On the application of statistical concepts to the buffeting problem. *J. Aeronau. Sci.*, 19, 793-800.

Peil, U., and Behrens, M. (2002). Fatigue of tubular steel lighting columns under wind load. *Wind and Struc.*, 5(5), 463-478.

Repetto, M. P., and Solari, G. (2004). Directional wind-induced fatigue of slender vertical structures. *J. Struct. Eng.*, 130(7), 1032-1040.

Rios, C (2007). Fatigue Performance of Multi-Sided High-Mast Lighting Towers. MATER'S Thesis, The University of Texas at Austin, Austin, Texas.

Scanlan, R. H. (1984). Role of indicial functions in buffeting analysis of bridges. *J. Struct. Eng.*, 110(7), 1433-1446.

Scanlan, R. H. (1993). Problematics in formulation of wind-force models for bridge decks. *J. Eng. Mech.*, 119(7), 1353-1375.

Scruton, C. (1981), An introduction to wind effects on structures, Engineering design guides 40, BSI&CEI.

Sears,W. R. (1941). Some aspects of non-stationary airfoil theory and its practical applications. *J. Aeronau. Sc.,* 8, 104-108.

Skop, R. A., and Griffin, O. M. (1975) On a theory for the vortex-excited oscillations of flexible cylindrical structures. *J. Sound Vib.*, 41, 263-274.

Simiu, E., and Scanlan, R. H. (1996). Wind Effects on Structures, Fundamentals and Applications to Design, 3rd ed., John Wiley & Sons, New York, NY.

Vickery, B. J. (1965). On the flow behind a coarse grid and its use as a model of atmospheric turbulence in studies related to wind loads on buildings, National Physical Laboratory Aero Report 1143.

Zhang, X., and Brownjohn, J. M. W. (2003). Time domain formulation of self-excited forces on bridge deck for wind tunnel experiment. *J. Wind. Eng. Ind. Aerodyn.*, 91, 723-736.

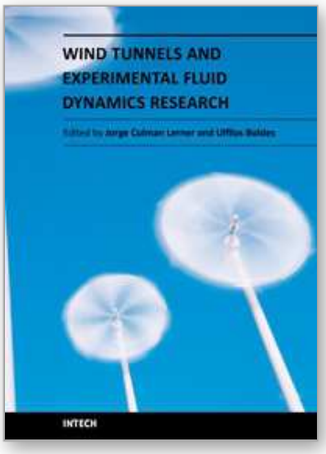

Wind Tunnels and Experimental Fluid Dynamics Research

Edited by Prof. Jorge Colman Lerner

ISBN 978-953-307-623-2

Hard cover, 709 pages

Publisher InTech

Published online 27, July, 2011

Published in print edition July, 2011

The book â€œWind Tunnels and Experimental Fluid Dynamics Researchâ€ is comprised of 33 chapters divided in five sections. The first 12 chapters discuss wind tunnel facilities and experiments in incompressible flow, while the next seven chapters deal with building dynamics, flow control and fluid mechanics. Third section of the book is dedicated to chapters discussing aerodynamic field measurements and real full scale analysis (chapters 20-22). Chapters in the last two sections deal with turbulent structure analysis (chapters 23-25) and wind tunnels in compressible flow (chapters 26-33). Contributions from a large number of international experts make this publication a highly valuable resource in wind tunnels and fluid dynamics field of research.

How to reference

In order to correctly reference this scholarly work, feel free to copy and paste the following:

Byungik Chang (2011). Aerodynamic Parameters on a Multisided Cylinder for Fatigue Design, Wind Tunnels and Experimental Fluid Dynamics Research, Prof. Jorge Colman Lerner (Ed.), ISBN: 978-953-307-623-2, InTech, Available from: http://www.intechopen.com/books/wind-tunnels-and-experimental-fluid-dynamics-research/aerodynamic-parameters-on-a-multisided-cylinder-for-fatigue-design

INTECH
open science | open minds

InTech Europe
University Campus STeP Ri
Slavka Krautzeka 83/A
51000 Rijeka, Croatia
Phone: +385 (51) 770 447
Fax: +385 (51) 686 166
www.intechopen.com

InTech China
Unit 405, Office Block, Hotel Equatorial Shanghai
No.65, Yan An Road (West), Shanghai, 200040, China
中国上海市延安西路65号上海国际贵都大饭店办公楼405单元
Phone: +86-21-62489820
Fax: +86-21-62489821